$X(1835)$, $X(2120)$, and $X(2370)$ in flux tube models

Chengrong Deng,[1] Jialun Ping,[2,*] Youchang Yang,[3] and Fan Wang[4]

[1]*School of Mathematics and Physics, Chongqing Jiaotong University, Chongqing 400074, People's Republic of China*
[2]*Department of Physics, Nanjing Normal University, Nanjing 210097, People's Republic of China*
[3]*Department of Physics, Zunyi Normal College, Zunyi 563002, People's Republic of China*
[4]*Department of Physics, Nanjing University, Nanjing 210093, People's Republic of China*

Nonstrange hexaquark state $q^3\bar{q}^3$ spectrum is systematically studied by using the Gaussian expansion method in flux tube models with a six-body confinement potential. All the model parameters are fixed by baryon properties, so the calculation of hexaquark state $q^3\bar{q}^3$ is parameter-free. It is found that some ground states of $q^3\bar{q}^3$ are stable against disintegrating into a baryon and an anti-baryon. The main components of $X(1835)$ and $X(2370)$, which are observed in the radiative decay of J/ψ by BES collaboration, can be described as compact hexaquark states $N_8\bar{N}_8$ and $\Delta_8\bar{\Delta}_8$ with quantum numbers $I^G J^{PC} = 0^+0^{-+}$, respectively. These bound states should be color confinement resonances with three-dimensional configurations similar to a rugby ball, however, $X(2120)$ can not be accommodated in this model approach.

I. INTRODUCTION

In 2003, $X(1860)$ was observed in the $p\bar{p}$ invariant mass spectrum in the radiative decay $J/\psi \rightarrow \gamma p\bar{p}$ by BES collaboration, the mass and the width are $M = 1859^{+3+5}_{-10-20}$ MeV and $\Gamma < 30$ MeV, respectively [1]. In 2005, $X(1835)$ was first observed in $J/\psi \rightarrow \gamma\pi^+\pi^-\eta'$ decays with a statistical significance of 7.7σ by BES-II [2], the parameters of $X(1835)$ are $M = 1833.7 \pm 6.5 \pm 2.7$ MeV and $\Gamma = 67.7 \pm 20.3 \pm 7.7$ MeV. Very recently, the $X(1835)$ was confirmed by BES-III in the radiative decay $J/\psi \rightarrow \gamma\pi^+\pi^-\eta'$ with mass and width $M = 1836.5 \pm 3.0^{+5.6}_{-2.1}$ MeV and $\Gamma = 190 \pm 9^{+38}_{-36}$ MeV, respectively [3]. The mass is consistent with the BES-II result, while the width is significantly larger. Meanwhile, $X(2120)$ and $X(2370)$ were also observed in the same process, the masses and the widths are $M_{X(2120)} = 2122.4 \pm 6.7^{+4.7}_{-2.7}$ MeV, $M_{X(2370)} = 2376.3 \pm 8.7^{+3.2}_{-4.3}$ MeV, $\Gamma_{X(2120)} = 83 \pm 16^{+31}_{-11}$ MeV, and $\Gamma_{X(2370)} = 83 \pm 17^{+44}_{-6}$ MeV, respectively.

Various theoretical works were stimulated to interpret the natures and structures of these resonances. Datta and O'Donnell described $X(1860)$ as a zero baryon number, deuteron-like singlet $p\bar{p}^0S_1$ state in a simple potential model with a $\lambda \cdot \lambda$ confining interaction [4]. Ding and Yan discussed $X(1860)$ as a baryonium and investigated mesonic decays of $X(1860)$ due to the nucleon-antinucleon annihilation [5]. Gao and Zhu understood $X(1860)$ as the $p\bar{p}$ bound state with quantum numbers $I^G J^{PC} = 0^+0^{-+}$ and demonstrated that it cannot decay into final state $\pi^+\pi^-$, $2\pi^0$, $\bar{K}K$ and 3π [6]. Kochelev and Min explained $X(1835)$ as the lowest pseudoscalar glueball state due to the instanton mechanism of partial $U(1)_A$ symmetry

restoration [7]. He *et al.*. studied $X(1835)$ using the QCD sum rule and interpreted it as a pseudoscalar state with a large gluon content [8]. Li investigated $X(1835)$ as a 0^{-+} pseudoscalar glueball using an effective Lagrangian approach [9]. Ding *et al.*. treated $X(1835)$ as a baryonium with a sizable gluon content [10]. Liu proposed that $X(1835)$ contained a baryonium component from the large-N_c QCD point of view [11]. Dedonder *et al.* studied $X(1835)$ in the conventional $N\bar{N}$ potential model and suggested that it could be a broad and weakly bound state $N\bar{N}_s(1870)$ in the $^1S_0$ wave. Huang and Zhu treated $X(1835)$ as the second radial excitation of $\eta'(958)$ and discussed the strong decay behavior by the effective Lagrangian approach [12]. Li and Ma studied several two-body strong decays of $X(1835)$ associated with $\eta(1760)$ by the quark-pair-creation model, where $X(1835)$ is assigned as the $n^{2s+1}L_J = 3^1S_0$ $q\bar{q}$ state. Entem and Fernández derived a $N\bar{N}$ interaction from a constituent quark model constrained by the NN sector to investigate the possible baryonium resonant state $X(1835)$ [13]. Yu *et al.*'s study indicated that: (i) $X(1835)$ could be the second radial excitation of $\eta'(958)$; (ii) $X(2120)$ and (2370) can be explained as the third and fourth radial excitations of $\eta(548)/\eta'(958)$ [14].

QCD is widely accepted as the fundamental theory to describe the hadron and the strong interaction and has verified in high momentum transfer process. In the low energy region, such as hadron spectroscopy and hadron-hadron interaction study, the *ab initio* calculation directly from QCD becomes very difficult due to the complication of nonperturbative nature. Recently, lattice QCD (LQCD) and nonperturbative QCD method have made impressive progresses on hadron properties, even on hadron-hadron interactions [15–19]. However, QCD-inspired constituent quark model (CQM) is still a useful tool in obtaining

*Corresponding author: jlping@njnu.edu.cn

physical insight for these complicated strong interaction systems. CQM can offer the most complete description of hadron properties and is probably the most successful phenomenological model of hadron structure [20]. In traditional CQM, a two-body interaction proportional to the color charges $\lambda_i \cdot \lambda_j$ and r_{ij}^n, where $n = 1$ or 2 and r_{ij} is the distance between two quarks, was introduced to phenomenologically describe quark confinement interaction. The model can automatically prevent overall color singlet multiquark states disintegrating into several color subsystems by means of color confinement with an appropriate $SU_C(3)$ Casimir constant [21]. The model also allows a multiquark system disintegrating into color-singlet clusters, and it leads to interacting potentials within mesonlike $q\bar{q}$ and baryonlike qqq subsystems in accord with the empirically known potentials [21]. However, the model is known to be flawed phenomenologically because it leads to power law van der Waals forces between color-singlet hadrons [22–26]. It is also flawed theoretically in that it is very implausible that the long-range static multibody potential is just a sum of the two-body ones [21]. The problems are related to the fact that this model does not respect local color gauge invariance [27–30]. Robson proposed to use many-body confinement potentials for meson-meson and baryon-baryon systems [30], which contains the essential features of the solution which emerges from the flux model based on the strong coupling limit of LQCD Hamiltonian and on the explicit local color gauge invariance [31].

QCD does not deny the existence of multiquark states although experimental candidates have not been confirmed up to now. The structures of multiquark systems and hadron-hadron interactions are abundant [32–34], which have important information that is absent in ordinary hadrons, such as $qq\bar{q}$ and $q\bar{q}\bar{q}$ interactions [35]. Recently, LQCD calculations on mesons, baryons, tetraquark, and pentaquark states reveal flux-tube or string like structure [36–39]. The confinement of multiquark states are multibody interactions and can be simulated by a potential which is proportional to the minimum of the total length of strings connecting the quarks to form a multiquark system. A naive flux-tube or string model basing on this picture has been constructed [32–34]. It takes into account multibody confinement with harmonic interaction approximation, i.e., where the length of string is replaced by the square of the length to simplify the numerical calculation. There are two arguments to support this approximation: One is that the spatial variations in separation of the quarks (lengths of the string) in different hadrons do not differ significantly, so the difference between the linear and quadratic forms is small and can be absorbed in the adjustable parameter, the stiffness. The calculations on nucleon-nucleon interactions support the argument [32,40,41]. The second is that we are using a nonrelativistic description of the dynamics and, as was shown long ago [42], an interaction energy that varies linearly with separation between

fermions in a relativistic, first order differential dynamics has a wide region in which a harmonic approximation is valid for the second order (Feynman-Gell-Mann) reduction of the equations of motion.

The flux tube model has been applied to the study of exotic mesons [33]. The results suggest that the multibody confinement should be employed in the quark model study of multiquark systems instead of the additive two-body confinement. The flux tube model with four-body confinement potential also described light scalar meson spectrum well in the framework of a tetraquark picture [43]. This paper extends the model to hexaquark $q^3\bar{q}^3$ system, to investigate systematically the non-strange baryonium states with six-body confinement potential. The numerical results are obtained by Gaussian expansion method (GEM) [44]. The paper is organized as follows: the model Hamiltonian and wave function for 3-quark system are presented in Sec. II. The six-body confinement potential and the wavefunction of a hexaquark system are introduced in Sec. III. Section IV presents the numerical results and discussions. A brief summary is given in the last section.

II. QUARK MODELS AND MODEL PARAMETERS

The nonrelativistic quark model was formulated under the assumption that the hadrons are color singlet nonrelativistic bound states of constituent quarks with phenomenological effective masses and interactions.

A. Isgur-Karl model

Isgur-Karl model incorporating effective one gluon exchange (OGE) and confinement potentials successfully describe the properties of baryon spectrum [45–47]. The model Hamiltonian used for baryons takes the form

$$H = \sum_{i=1}^{3}\left(m_i + \frac{\mathbf{p}_i^2}{2m_i}\right) - T_{CM} + \sum_{i>j}^{3} V_{ij}^G + V^C, \quad (1)$$

$$V_{ij}^G = \frac{1}{4}\alpha_s \lambda_i \cdot \lambda_j \left[\frac{1}{r_{ij}} - \frac{\pi}{2}\delta(\mathbf{r}_{ij})\left(\frac{1}{m_i^2} + \frac{1}{m_j^2} + \frac{4}{3m_im_j}\sigma_i \cdot \sigma_j\right)\right], \quad (2)$$

$$V^C = \frac{K}{3}\left[(\mathbf{r}_1 - \mathbf{r}_2)^2 + (\mathbf{r}_1 - \mathbf{r}_3)^2 + (\mathbf{r}_2 - \mathbf{r}_3)^2\right], \quad (3)$$

the confinement potential V^C can also be written as

$$V^C = K\left[\left(\frac{\mathbf{r}_1 - \mathbf{r}_2}{\sqrt{2}}\right)^2 + \left(\frac{\mathbf{r}_1 + \mathbf{r}_2 - 2\mathbf{r}_3}{\sqrt{6}}\right)^2\right]. \quad (4)$$

When the model is extended to study multiquark states [48], the confinement can be equivalently expressed as

$$V^C = \sum_{i>j}^{n} -a_c \lambda_i \cdot \lambda_j r_{ij}^2. \quad (5)$$

Where T_{CM} is the center-of-mass kinetic energy, $\mathbf{r}_i$, m_i, and $\mathbf{p}_i$ are the position, mass and momentum of the ith quark, λ and $\boldsymbol{\sigma}$ are the $SU(3)$ Gell-Mann and $SU(2)$ Pauli matrices, respectively. Note that $\lambda \to -\lambda^*$ for antiquark. All other symbols have their usual meaning. An effective scale-dependent strong coupling constant [49] is used here

$$\alpha_s(\mu) = \frac{\alpha_0}{\ln\left[\frac{\mu^2 + \mu_0^2}{\Lambda_0^2}\right]}, \tag{6}$$

where μ is the reduced mass of two interactional quarks, and α_0, μ_0, and Λ_0 are determined below. The δ function, arising as a consequence of the nonrelativistic reduction of the one-gluon exchange diagram between point-like particles, has to be regularized in order to perform numerical calculations. It reads [50]

$$\delta(r_{ij}) = \frac{1}{\beta^3 \pi^{(3/2)}} e^{-r_{ij}^2/\beta^2}, \tag{7}$$

where β is the model parameter which is determined by fitting the experiment data.

B. Chiral quark model

The $SU(2) \times SU(2)$ chiral quark model described NN phase shifts and the properties of deuteron quite well [51–53]. Subsequently, the $SU(3) \times SU(3)$ chiral quark model where constituent quarks interact only through pseudoscalar Goldstone bosons exchange (GBE) was developed to describe the baryon spectra [54]. The model including both OGE and GBE was successfully applied to the NN and nucleon-hyperon interactions [55–57]. The Goldstone bosons exchange potentials can be expressed as,

$$V_{ij}^B = v_{ij}^\pi \sum_{a=1}^3 \mathbf{F}_i^a \mathbf{F}_j^a + v_{ij}^K \sum_{a=4}^7 \mathbf{F}_i^a \mathbf{F}_j^a \\ + v_{ij}^\eta (\mathbf{F}_i^8 \mathbf{F}_j^8 \cos\theta_P - \mathbf{F}_i^0 \mathbf{F}_j^0 \sin\theta_P), \tag{8}$$

$$v_{ij}^\chi = \frac{g_{ch}^2}{4\pi} \frac{m_\chi^3}{12 m_i m_j} \frac{\Lambda_\chi^2}{\Lambda_\chi^2 - m_\chi^2} \boldsymbol{\sigma}_i \cdot \boldsymbol{\sigma}_j \\ \times \left[Y(m_\chi r_{ij}) - \frac{\Lambda_\chi^3}{m_\chi^3} Y(\Lambda_\chi r_{ij}) \right], \tag{9}$$

$$\chi = \pi, K, \eta,$$

$$V_{ij}^\sigma = -\frac{g_{ch}^2}{4\pi} \frac{\Lambda_\sigma^2}{\Lambda_\sigma^2 - m_\sigma^2} m_\sigma \left[Y(m_\sigma r_{ij}) - \frac{\Lambda_\sigma}{m_\sigma} Y(\Lambda_\sigma r_{ij}) \right],$$

where $Y(x)$ is the standard Yukawa functions defined by $Y(x) = \frac{e^{-x}}{x}$ and $\mathbf{F}^a$ is flavor $SU(3)$ Gell-Mann matrices. The angle θ_P appears as a consequence of considering the physical η instead of the octet one. m_π, m_K, and m_η are the masses of the $SU(3)$ Goldstone bosons, took their experimental values. m_σ is determined through the PCAC relation $m_\sigma^2 \sim m_\pi^2 + 4m_{u,d}^2$ [58]. The chiral coupling constant

g_{ch} is determined from the πNN coupling constant through

$$\frac{g_{ch}^2}{4\pi} = \left(\frac{3}{5}\right)^2 \frac{g_{\pi NN}^2}{4\pi} \frac{m_{u,d}^2}{m_N^2}. \tag{10}$$

Here the flavor $SU(3)$ is assumed to be an exact system and only broken by the different mass of the strange quark. The confinement and OGE interaction terms are the same as those of the Isgur-Karl model and will not be rewritten here.

C. Flux-tube model

This model assumption is inspired by the LQCD calculation. LQCD calculations for baryons reveal flux-tube or string like structure [37,59]. The simplified version, Y-shape structure, is shown in Fig. 1, where the $\mathbf{r}_i$ represents the spatial position of the ith quark denoted by a black dot and $\mathbf{y}_0$ denotes the junction where three color flux tubes meet. The confinement is proportional to the minimum of the sum of the square of the length of three flux tubes. In the flux tube model with quadratic potential, the three-body confinement can be written as

$$V^C = K[(\mathbf{r}_1 - \mathbf{y}_0)^2 + (\mathbf{r}_2 - \mathbf{y}_0)^2 + (\mathbf{r}_3 - \mathbf{y}_0)^2]. \tag{11}$$

For the confinement potential V^C, the position of the junction $\mathbf{y}_0$ can be fixed by minimizing the energy of the system, then we get

$$\mathbf{y}_0 = \frac{\mathbf{r}_1 + \mathbf{r}_2 + \mathbf{r}_3}{3}. \tag{12}$$

Therefore, the minimum of the confinement potential for baryons $V_{\min}^C$ has the following forms

$$V_{\min}^C = K\left[\left(\frac{\mathbf{r}_1 - \mathbf{r}_2}{\sqrt{2}}\right)^2 + \left(\frac{2\mathbf{r}_3 - \mathbf{r}_1 - \mathbf{r}_2}{\sqrt{6}}\right)^2\right]. \tag{13}$$

The other parts of the Hamiltonian of the flux tube model are the same as the Isgur-Karl model (denoted as Model I hereafter) or chiral quark model (Model II). It should be noted that for a baryon the three-body quadratic confinement potential is exactly equivalent to the sum of two-body one, Δ-shape in Fig. 1 (although it is not exactly the case for the linear confinement potential). As far as baryon is concerned, the flux tube model is not a new model. However, when it is applied to multiquark systems, the
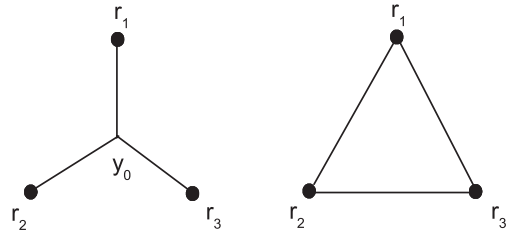

FIG. 1.   Three-body and two-body confinement potential.

flux-tube confinement potential is different from the traditional two-body confinement ((Isgur-Karl model and chiral quark model) [32–34].

In this work, the tensor forces and spin-orbit forces between quarks are omitted in three models, because of their small or zero contributions to the ground state baryons.

D. Wave functions and baryon spectrums

For baryons, the color part wave function ψ_c is antisymmetrical because of the color singlet requirement. The spatial wave function $\psi^G_{L_T M_T}(\mathbf{R}, \mathbf{r})$ is assumed to be symmetrical because we are interested in ground states. So the spin-flavor wave function $\psi_{IM_I SM_S}$, the $SU(6) \supset SU_s(2) \times SU_f(3)$ symmetry is used here, is symmetrical under the exchange of two identical particles. The total antisymmetrical wave function can be described as

$$\Phi_{IM_I JM_J}(\mathbf{R}, \mathbf{r}) = \psi_c \Big[\psi^G_{L_T M_T}(\mathbf{R}, \mathbf{r}) \psi_{IM_I SM_S} \Big]_{IM_I JM_J}. \quad (14)$$

$[\cdots]_{IM_I JM_J}$ means coupling the spin S and total orbital angular momentum L_T with Clebsch-Gordan coefficients.

We define Jacobi coordinates $\mathbf{r}_{ij}$ and $\mathbf{R}_k$ for the cyclic permutations of (1, 2, 3),

$$\mathbf{r}_{ij} = \mathbf{r}_i - \mathbf{r}_j, \qquad \mathbf{R}_k = \mathbf{r}_k - \frac{m_i \mathbf{r}_i + m_j \mathbf{r}_j}{m_i + m_j}. \quad (15)$$

Then, the spatial symmetrical wave functions can be expressed as

$$\Psi_{L_T M_T}(\mathbf{R}, \mathbf{r}) = \sum_{i,j,k=1}^{3} \big[\phi_{lm}(\mathbf{r}_{ij}) \phi_{LM}(\mathbf{R}_k) \big]_{L_T M_T}. \quad (16)$$

$\phi_{lm}(\mathbf{r}_{ij})$ and $\phi_{LM}(\mathbf{R}_k)$ are the superpositions of Gaussian basis functions with different sizes,

$$\phi_{lm}(\mathbf{r}_{ij}) = \sum_{n=1}^{n_{\max}} c_n N_{nl} r_{ij}^l e^{-\nu_n r_{ij}^2} Y_{lm}(\hat{\mathbf{r}}_{ij}), \quad (17)$$

$$\psi_{LM}(\mathbf{R}_k) = \sum_{N=1}^{N_{\max}} c_N N_{NL} R_k^L e^{-\nu_N R_k^2} Y_{LM}(\hat{\mathbf{R}}_k), \quad (18)$$

where N_{nl} and N_{NL} are normalization constants. Gaussian size parameters ν_n and ν_N are taken as geometric progression,

$$r_n = r_1 a^{n-1}, \qquad \nu_n = \frac{1}{r_n^2}, \qquad a = \left(\frac{r_{n_{\max}}}{r_1} \right)^{1/n_{\max}-1}, \quad (19)$$

$$R_N = R_1 A^{N-1}, \qquad \nu_N = \frac{1}{R_N^2}, \qquad A = \left(\frac{R_{N_{\max}}}{R_1} \right)^{1/N_{\max}-1}. \quad (20)$$

The numbers n and l (N and L) specify the radial and angular momenta excitations with respect to the Jacobi coordinates $\mathbf{r}$ ($\mathbf{R}$), respectively. The angular momenta l and L are coupled to the total orbit angular momentum L_T. In the present work all three angular momenta are assumed to be zero.

Using the above Hamiltonian and wave functions, the light baryon spectra and the corresponding model parameters can be obtained by solving the three-body Schrödinger equation

$$(H_3 - E)\Phi_{IM_I JM_J}(\mathbf{R}, \mathbf{r}) = 0 \quad (21)$$

with Rayleigh-Ritz variational principle. The converged results, which are shown in Table I, are arrived by setting $r_1 = R_1 = 0.3$ fm, $r_{n_{\max}} = R_{n_{\max}} = 2.0$ fm and $n_{\max} = N_{\max} = 5$. It can be seen from Table I that Isgur-Karl model and chiral quark model give similar numerical results, which can describe well the light baryon spectrum. The fitting parameters in the Isgur-Karl model and chiral quark model are listed in Table II, in which five parameters are readjusted to fit the light baryon spectrum. Other parameters Λ_π, Λ_σ, Λ_η, Λ_K, θ_P, Λ_0, and μ_0, which are fixed by fitting the meson spectra, are taken from Ref. [49].

III. SIX-BODY CONFINEMENT POTENTIALS IN THE FLUX TUBE MODEL

In the flux tube model it is assumed that the color-electric flux is confined to narrow, string-like tubes joining quarks. A flux tube starts from every quark and ends at an antiquark or a Y-shaped junction, where three flux tubes annihilate or are created [60]. In general, a state with $N + 1$-particles can be generated by replacing a quark or an antiquark in an N-particles state by a Y-shaped junction and two quarks or two antiquarks.

The $q^3 \bar{q}^3$ systems have been studied in the usual constituent quark model including a two-body confinement potential proportional to a color factor, no bound state is found for a non-strange system [61,60]. Vijande *et al.*.

TABLE I. Baryon spectra (unit: MeV).

State	N	Λ	Σ	Ξ	Δ	Σ^*	Ξ^*	Ω
Isgur-Karl	939	1022	1196	1307	1232	1397	1542	1673
Chiral	939	1048	1249	1375	1232	1391	1536	1670
Experiment	939	1116	1195	1315	1232	1384	1533	1672

TABLE II.   Model parameters.

Classification	Parameters	Isgur-Karl	Chiral
		(Model I)	(Model II)
Readjusted	m_{ud} (MeV)	313	360
	m_s (MeV)	585	560
	K (MeV fm^{-2})	336	224
	β (fm)	0.32	0.08
	α_0	6.82	5.21
	Λ_0 (fm^{-1})	0.187	0.187
	μ_0 (fm^{-1})	0.113	0.113
	Λ_π (fm^{-1})	...	4.2
	Λ_σ (fm^{-1})	...	4.2
	Λ_K (fm^{-1})	...	5.2
Fixed	Λ_η (fm^{-1})	...	5.2
	m_π (fm^{-1})	...	0.70
	m_K (fm^{-1})	...	2.51
	m_η (fm^{-1})	...	2.77
	m_σ (fm^{-1})	...	3.72
	θ_P (o)	...	-15
	$g_{ch}^2/4\pi$	...	0.54

recently studied the stability of hexaquark states (q^6 and $q^3\bar{q}^3$) in the string confinement and found that the ground states of $Q^3\bar{q}^3$ are stable against disintegrating into two color singlet baryons [61]. For $q^3\bar{q}^3$ system, it can be consisted of a color singlet baryon and a color singlet antibaryon as in the usual hadron degree of freedom description, but also of a color octet baryon and a color octet antibaryon coupled to an overall color singlet six quark state. The former is named as hadronic molecule state, the latter is called hidden color channel and because of color confinement, the hidden color channel exists in the two-cluster overlap region only. These two structures are shown in Figs. 2 and 3, respectively. In general, a hexaquark system $q^3\bar{q}^3$ should be a mixture of these two components. These two structures for $q^3\bar{q}^3$ system are considered in the present work.

In Figs. 2 and 3, $\mathbf{r}_\alpha$ represents the position coordinate of the quark q_α (antiquark $\bar{q}_\alpha$) which is denoted by a solid (hollow) dot, where $\alpha = i, \ldots, n$, (i, j, k) and (l, m, n) are cyclic indexes for $(1, 2, 3)$ and $(4, 5, 6)$, respectively. $\mathbf{y}_\beta$ represents a junction, where $\beta = 1, \ldots, 4$. A thin line connecting a quark and a junction represents a fundamental
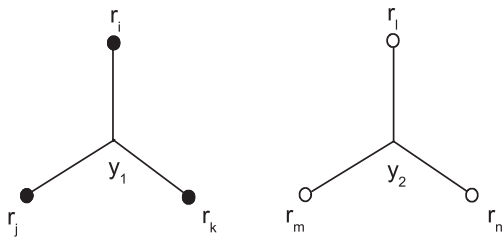
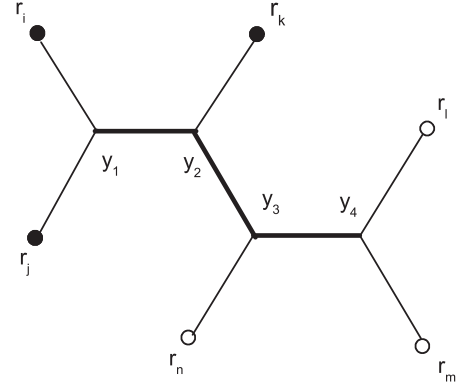

FIG. 2.   Hadronic molecule structure.

FIG. 3.   Hidden color flux tube structure.

string, i.e., a color triplet, a thick line connecting two junctions is for color sextet, octet or others, namely a compound string.

Within the flux tube model, the confinement potential for a hadronic molecule state can be written as

$$V_{\min}^{CM} = K\left[\left(\frac{\mathbf{r}_i - \mathbf{r}_j}{\sqrt{2}}\right)^2 + \left(\frac{2\mathbf{r}_k - \mathbf{r}_i - \mathbf{r}_j}{\sqrt{6}}\right)^2 + \left(\frac{\mathbf{r}_l - \mathbf{r}_m}{\sqrt{2}}\right)^2 + \left(\frac{2\mathbf{r}_n - \mathbf{r}_l - \mathbf{r}_m}{\sqrt{6}}\right)^2\right].$$

(22)

With respect to a hidden color state, the confinement potential has the following form:

$$\begin{aligned}
V^{CH} = K[&(\mathbf{r}_i - \mathbf{y}_1)^2 + (\mathbf{r}_j - \mathbf{y}_1)^2 + (\mathbf{r}_k - \mathbf{y}_2)^2 \\
&+ (\mathbf{r}_n - \mathbf{y}_3)^2 + (\mathbf{r}_l - \mathbf{y}_4)^2 + (\mathbf{r}_m - \mathbf{y}_4)^2 \\
&+ \kappa_{d_{12}}(\mathbf{y}_1 - \mathbf{y}_2)^2 + \kappa_{d_{23}}(\mathbf{y}_2 - \mathbf{y}_3)^2 + \kappa_{d_{34}}(\mathbf{y}_3 - \mathbf{y}_4)^2].
\end{aligned}$$

(23)

The string stiffness constant of an elementary or color triplet string is K, while $K\kappa_{d_{ij}}$ is other compound string stiffness. The compound string stiffness parameter $\kappa_{d_{ij}}$ [62] depends on the color dimension, d_{ij}, of the string,

$$\kappa_{d_{ij}} = \frac{C_{d_{ij}}}{C_3},$$

(24)

where $C_{d_{ij}}$ is the eigenvalue of the Casimir operator associated with the $SU(3)$ color representation d_{ij} on either end of the string, namely $C_3 = \frac{4}{3}$, $C_6 = \frac{10}{3}$, and $C_8 = 3$. In numerical calculations, the average κ_d for $\kappa_{d_{ij}}$ is used for simplicity.

For given quark (antiquark) positions $\mathbf{r}_\alpha$, those junction coordinates $\mathbf{y}_\beta$ are obtained by minimizing the confinement potential. By introducing the following set of canonical coordinates $\mathbf{R}_i$,

$$\mathbf{R}_1 = \frac{1}{\sqrt{2}}(\mathbf{r}_i - \mathbf{r}_j), \qquad \mathbf{R}_2 = \frac{1}{\sqrt{2}}(\mathbf{r}_l - \mathbf{r}_m),$$

$$\mathbf{R}_3 = \frac{1}{\sqrt{12}}(\mathbf{r}_i + \mathbf{r}_j - 2\mathbf{r}_k - 2\mathbf{r}_n + \mathbf{r}_l + \mathbf{r}_m),$$

$$\mathbf{R}_4 = \frac{1}{\sqrt{33 + 5\sqrt{33}}}(\mathbf{r}_i + \mathbf{r}_j - w_1\mathbf{r}_k + w_1\mathbf{r}_n - \mathbf{r}_l - \mathbf{r}_m),$$

$$\mathbf{R}_5 = \frac{1}{\sqrt{33 - 5\sqrt{33}}}(\mathbf{r}_i + \mathbf{r}_j + w_2\mathbf{r}_k - w_2\mathbf{r}_n - \mathbf{r}_l - \mathbf{r}_m),$$

$$\mathbf{R}_6 = \frac{1}{\sqrt{6}}(\mathbf{r}_i + \mathbf{r}_j + \mathbf{r}_k + \mathbf{r}_l + \mathbf{r}_m + \mathbf{r}_n), \qquad (25)$$

where $w_1 = \frac{\sqrt{33}+5}{2}$ and $w_2 = \frac{\sqrt{33}-5}{2}$, the minimum of the confinement potential takes the following form,

$$V_{\min}^{CH} = K\Bigg[\mathbf{R}_1^2 + \mathbf{R}_2^2 + \frac{3\kappa_d}{2 + 3\kappa_d}\mathbf{R}_3^2$$
$$+ \frac{2\kappa_d(\kappa_d + w_3)}{2\kappa_d^2 + 7\kappa_d + 2}\mathbf{R}_4^2 + \frac{2\kappa_d(\kappa_d + w_4)}{2\kappa_d^2 + 7\kappa_d + 2}\mathbf{R}_5^2 \Bigg], \quad (26)$$

where $w_3 = \frac{7+\sqrt{33}}{4}$ and $w_4 = \frac{7-\sqrt{33}}{4}$. Clearly this confinement potential is multibody interaction rather than the sum of a two-body one in the sense that a move of a quark may affect the flux tubes connecting pattern.

When two clusters q^3 and $\bar{q}^3$ separate in a long distance, a baryon and an antibaryon should be a dominant component of a hexaquark $q^3\bar{q}^3$ system because other hidden color flux tube structures are suppressed due to the confinement. On the other hand, if the separation is intermediate, a hadronic molecule state may be formed if the attractive force between a baryon and an antibaryon is strong enough. When the two quark-clusters are close enough to be within the range of confinement (about 1 fm), all possible flux tube structures will appear due to the excitation and rearrangement of flux tubes. In this case, the confinement potential of a hexaquark system $q^3\bar{q}^3$ should be taken to be the minimum of two flux tube structures. It reads

$$V_{\min}^C = \min[V_{\min}^{CM}, V_{\min}^{CH}]. \qquad (27)$$

IV. NUMERICAL RESULTS AND DISCUSSIONS

The flux tube structure specifies how the colors of quarks and antiquarks are coupled to form an overall color singlet. Therefore, the model wave function with defined quantum numbers I_T and J_T can be expressed as

$$\Psi_{I_T,J_T}^{q^3\bar{q}^3} = \sum c_\xi [[\Phi_{c_1 IJ}^{q^3} \Phi_{c_2 I'J'}^{\bar{q}^3}]_\xi F_{L'}(\mathbf{X})]_{I_T J_T}. \qquad (28)$$

$\Phi_{c_1 IJ}^{q^3}$ and $\Phi_{c_2 I'J'}^{\bar{q}^3}$ are cluster wave functions of colorful or colorless baryon and anti-baryon, respectively. The spatial wave functions are the same as those of baryons shown before, $[\cdots]_\xi$ represents all the needed coupling: color, isospin, and spin coupling. $F_{L'}(\mathbf{X})$ is the relative orbital

wave function between q^3 and $\bar{q}^3$ clusters. All the possible channels are taken into account in our multichannel coupling calculation, the details can be seen in Table III. The Jacobi coordinates for a $q^3\bar{q}^3$ system are shown in Fig. 4, which can be expressed as

$$\mathbf{r}_{ij} = \mathbf{r}_i - \mathbf{r}_j, \qquad \mathbf{R}_k = \mathbf{r}_k - \frac{\mathbf{r}_i + \mathbf{r}_j}{2},$$

$$\mathbf{r}_{lm} = \mathbf{r}_l - \mathbf{r}_m, \qquad \mathbf{R}_n = \mathbf{r}_n - \frac{\mathbf{r}_l + \mathbf{r}_m}{2}, \qquad (29)$$

$$\mathbf{X} = \frac{\mathbf{r}_i + \mathbf{r}_j + \mathbf{r}_k}{3} - \frac{\mathbf{r}_l + \mathbf{r}_m + \mathbf{r}_n}{3}.$$

Using GEM, the relative orbital wave function $F_{L'}(\mathbf{X})$ can be written as

$$F_{L'}(\mathbf{X}) = \sum_{N'=1}^{N'_{\max}} c_{N'} N_{N'L'} X^{L'} e^{-\nu_{N'} X^2} Y_{L'M'}(\hat{\mathbf{X}}). \qquad (30)$$

Now we turn to the numerical calculations on $q^3\bar{q}^3$ systems. In Model I and II, where a six-body confinement potential is used, all the model parameters are fixed by fitting the ground state baryon spectrum, no new parameter is introduced in the six-body calculation. The eigenvalues and eigenfunctions of the $q^3\bar{q}^3$ states can be obtained by solving the following six-body Schrödinger equation

$$(H_6 - E)\Psi_{I_T J_T}^{q^3\bar{q}^3} = 0, \qquad (31)$$

with Rayleigh-Ritz variational principle. The calculated results are converged with $n_{\max} = 5$, $N_{\max} = 5$, and $N'_{\max} = 5$. Minimum and maximum ranges of the bases are 0.3 fm and 2.0 fm for coordinates $\mathbf{r}$, $\mathbf{R}$, and $\mathbf{X}$, respectively.

The lowest multichannel coupling results for all possible quantum numbers are listed in Table III, the superscript and subscript of $N(\Delta)$ represent spin quantum number and color dimensions, respectively. $E_T(B + \bar{B})$ is the threshold of decaying into a baryon and an antibaryon, ΔE_I and ΔE_{II} are binding energies of hexaquark states $q^3\bar{q}^3$ in Model I and Model II, respectively. It can be seen from Table III that the states with $I^G J^{PC} = 0^- 3^{--}$, $1^+ 3^{--}$, and $3^+ 1^{--}$ are bound states only in Model II. For other states almost the same qualitative results are obtained in two models. It suggests that there are some bound states below the lowest threshold in the present calculations. The states with $I^G J^{PC} = 0^+ 0^{-+}$ and $1^- 0^{-+}$ are stable against disintegrating into $N + \bar{N}$. The states with $I^G J^{PC} = 1^- 2^{-+}$, $2^- 1^{--}$, and $2^+ 2^{-+}$ are stable against disintegrating into $N + \bar{\Delta}$ or $\bar{N} + \Delta$, but decay to $N\bar{N}\pi$ is allowed. The states with $I^G J^{PC} = 0^+ 2^{-+}$, $2^+ 0^{-+}$, and $3^+ 0^{-+}$ are stable against disintegrating into $\Delta + \bar{\Delta}$, decaying to $N\bar{N}\pi\pi$ is allowed. The states with $I^G J^{PC} = 0^- 1^{--}$, $1^+ 1^{--}$, $2^- 3^{--}$, $3^- 2^{-+}$, and $3^+ 3^{--}$ states are not bound both in two models. The multibody confinement potential based on the color flux tube picture can give more attraction than the additive two-body confinement interaction which is proportional

TABLE III. Binding energies of lowest $q^3\bar{q}^3$ states with all possible quantum numbers in Model I and II. (unit: MeV).

$I^G J^{PC}$	Coupled channels	$E_T(B+\bar{B})$	ΔE_I	ΔE_{II}
0^+0^{-+}	$N_8^{1/2}\bar{N}_8^{1/2}$, $\Delta_8^{1/2}\bar{\Delta}_8^{1/2}$, $N_8^{3/2}\bar{N}_8^{3/2}$, $N\bar{N}$, $\Delta\bar{\Delta}$	$939+939$	-44	-34
0^-1^{--}	$N_8^{1/2}\bar{N}_8^{1/2}$, $N_8^{1/2}\bar{N}_8^{3/2}$, $\Delta_8^{1/2}\bar{\Delta}_8^{1/2}$, $N_8^{3/2}\bar{N}_8^{1/2}$, $N_8^{3/2}\bar{N}_8^{3/2}$, $N\bar{N}$, $\Delta\bar{\Delta}$	$939+939$	0	0
0^+2^{-+}	$N_8^{1/2}\bar{N}_8^{3/2}$, $N_8^{3/2}\bar{N}_8^{1/2}$, $N_8^{3/2}\bar{N}_8^{3/2}$, $\Delta\bar{\Delta}$	$1232+1232$	-269	-200
0^-3^{--}	$N_8^{2/2}\bar{N}_8^{3/2}$, $\Delta\bar{\Delta}$	$1232+1232$	0	-58
1^-0^{-+}	$N_8^{1/2}\bar{N}_8^{1/2}$, $N_8^{1/2}\bar{\Delta}_8^{1/2}$, $\Delta_8^{1/2}\bar{N}_8^{1/2}$, $\Delta_8^{1/2}\bar{\Delta}_8^{1/2}$, $N_8^{3/2}\bar{N}_8^{3/2}$, $N\bar{N}$, $\Delta\bar{\Delta}$	$939+939$	-44	-5
1^+1^{--}	$N_8^{1/2}\bar{N}_8^{1/2}$, $N_8^{1/2}\bar{\Delta}_8^{1/2}$, $N_8^{1/2}\bar{N}_8^{3/2}$, $\Delta_8^{1/2}\bar{N}_8^{1/2}$, $\Delta_8^{1/2}\bar{\Delta}_8^{1/2}$, $\Delta_8^{1/2}\bar{N}_8^{3/2}$, $N_8^{3/2}\bar{N}_8^{1/2}$, $N_8^{3/2}\bar{\Delta}_8^{1/2}$, $N_8^{3/2}\bar{N}_8^{3/2}$, $N\bar{N}$, $N\bar{\Delta}$, $\Delta\bar{N}$, $\Delta\bar{\Delta}$	$939+939$	0	0
1^-2^{-+}	$N_8^{1/2}\bar{N}_8^{3/2}$, $\Delta_8^{1/2}\bar{N}_8^{3/2}$, $N_8^{3/2}\bar{N}_8^{1/2}$, $N_8^{3/2}\bar{\Delta}_8^{1/2}$, $N_8^{3/2}\bar{N}_8^{3/2}$, $N\bar{\Delta}$, $\Delta\bar{N}$, $\Delta\bar{\Delta}$	$939+1232$	-7	-71
1^+3^{--}	$N_8^{3/2}\bar{N}_8^{3/2}$, $\Delta\bar{\Delta}$	$1232+1232$	0	-44
2^+0^{-+}	$N_8^{1/2}\bar{\Delta}_8^{1/2}$, $\Delta_8^{1/2}\bar{N}_8^{1/2}$, $\Delta_8^{1/2}\bar{\Delta}_8^{1/2}$, $\Delta\bar{\Delta}$	$1232+1232$	-88	-87
2^-1^{--}	$N_8^{1/2}\bar{\Delta}_8^{1/2}$, $\Delta_8^{1/2}\bar{N}_8^{1/2}$, $\Delta_8^{1/2}\bar{\Delta}_8^{1/2}$, $\Delta_8^{1/2}\bar{N}_8^{3/2}$, $N_8^{3/2}\bar{\Delta}_8^{1/2}$, $N\bar{\Delta}$, $\Delta\bar{N}$, $\Delta\bar{\Delta}$	$939+1232$	-13	-108
2^+2^{-+}	$N_8^{3/2}\bar{\Delta}_8^{1/2}$, $\Delta_8^{1/2}\bar{N}_8^{3/2}$, $N\bar{\Delta}$, $\Delta\bar{N}$, $\Delta\bar{\Delta}$	$939+1232$	-7	-34
2^-3^{--}	$\Delta\bar{\Delta}$	$1232+1232$	0	0
3^-0^{-+}	$\Delta_8^{1/2}\bar{\Delta}_8^{1/2}$, $\Delta\bar{\Delta}$	$1232+1232$	-88	-76
3^+1^{--}	$\Delta_8^{1/2}\bar{\Delta}_8^{1/2}$, $\Delta\bar{\Delta}$	$1232+1232$	0	-67
3^-2^{-+}	$\Delta\bar{\Delta}$	$1232+1232$	0	0
3^+3^{--}	$\Delta\bar{\Delta}$	$1232+1232$	0	0

to color factors used in early multiquark state calculations, due to avoiding the appearance of the anti-confinement in a color symmetrical quark or antiquark pair. In fact one gluon exchange and one boson exchange interaction also provide attractive interaction for some states [61].
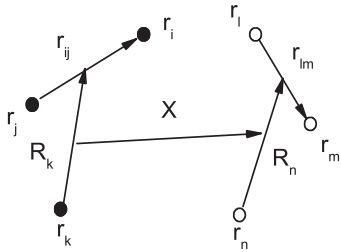
FIG. 4.   Jacobi ordinates for a $q^3\bar{q}^3$ system.

For the state $I^G J^{PC} = 0^+0^{-+}$, the wave function can be separated into two groups, $N\bar{N} + N_8\bar{N}_8$ and $\Delta\bar{\Delta} + \Delta_8\bar{\Delta}_8$. In Model I, there is no interaction between $N\bar{N} + N_8\bar{N}_8$ and $\Delta\bar{\Delta} + \Delta_8\bar{\Delta}_8$ due to the absence of a boson exchange term. The states $N\bar{N} + N_8\bar{N}_8$ and $\Delta\bar{\Delta} + \Delta_8\bar{\Delta}_8$ have the lowest energies 1834 MeV and 2376 MeV, respectively. However, $N\bar{N} + N_8\bar{N}_8$ and $\Delta\bar{\Delta} + \Delta_8\bar{\Delta}_8$ are mixed in Model II because there is interaction among them due to one boson exchange. But the mixing effect is not large. The energies of $N\bar{N} + N_8\bar{N}_8$ and $\Delta\bar{\Delta} + \Delta_8\bar{\Delta}_8$ are 1865 MeV and 2384 MeV in the Model II if the mixing effect among two groups is neglected. The mixing moves the energies of $N\bar{N} + N_8\bar{N}_8$ to 1844 MeV and $\Delta\bar{\Delta} + \Delta_8\bar{\Delta}_8$ to 2388 MeV. $N\bar{N} + N_8\bar{N}_8$ and $\Delta\bar{\Delta} + \Delta_8\bar{\Delta}_8$ are bound states because their energies are lower than the corresponding thresholds of $N\bar{N}$ and $\Delta\bar{\Delta}$ in these two models. The masses of

TABLE IV.   Rms for $N\bar{N} + N_8\bar{N}_8$ and $\Delta\bar{\Delta} + \Delta_8\bar{\Delta}_8$ (fm).

Model	Distances	$\langle \mathbf{R}_{qqq}{}^2\rangle^{1/2}$	$\langle \mathbf{R}_{\bar{q}\bar{q}\bar{q}}{}^2\rangle^{1/2}$	$\langle \mathbf{X}^2\rangle^{1/2}$
Model I	$N\bar{N} + N_8\bar{N}_8$	0.61	0.61	0.51
	$\Delta\bar{\Delta} + \Delta_8\bar{\Delta}_8$	0.65	0.65	0.60
Model II	$N\bar{N} + N_8\bar{N}_8$	0.66	0.66	0.58
	$\Delta\bar{\Delta} + \Delta_8\bar{\Delta}_8$	0.71	0.71	0.66

$N\bar{N} + N_8\bar{N}_8$ and $\Delta\bar{\Delta} + \Delta_8\bar{\Delta}_8$ states are close to the masses of newly observed states $X(1835)$ and $X(2370)$, so it is possible to interpret the main components of $X(1835)$ and $X(2370)$ as $N\bar{N} + N_8\bar{N}_8$ and $\Delta\bar{\Delta} + \Delta_8\bar{\Delta}_8$ in the present calculation, respectively. However, another state $X(2120)$ observed by BES-III cannot be described in the present calculations.

Using the wave functions of $N\bar{N} + N_8\bar{N}_8$ and $\Delta\bar{\Delta} + \Delta_8\bar{\Delta}_8$, the root mean square radii (rms) of the two states with $I^G J^{PC} = 0^+ 0^{-+}$ are calculated and given in Table IV, where

$$\mathbf{R}_{qqq} = \mathbf{r}_i - \frac{\mathbf{r}_i + \mathbf{r}_j + \mathbf{r}_k}{3}$$

and

$$\mathbf{R}_{\bar{q}\bar{q}\bar{q}} = \mathbf{r}_l - \frac{\mathbf{r}_l + \mathbf{r}_m + \mathbf{r}_n}{3}.$$

It can be seen from Table IV that the radii are small and very close in two models. The two clusters q^3 and $\bar{q}^3$ are highly overlapped, therefore the main components of $X(1835)$ and $X(2370)$ are not loose hadronic molecule states but compact hexaquark states with three-dimensional configurations similar to a rugby ball in the present calculations.

All hidden color components cannot decay into two colorful hadrons directly due to color confinement. $X(1835)$ and $X(2370)$ must transform back into three color singlet mesons by means of breaking and rejoining flux tubes before decaying into $\eta' \pi^+ \pi^-$. This decay mechanism is similar to compound nucleus formation and therefore should induce a resonance which is named as a "color confined, multiquark resonance" state [63] in our models. It is different from all of those microscopic resonances discussed by S. Weinberg [64]. Bicudo and Cardoso studied tetraquark states using the triple flip-flop potential including two meson-meson potentials and the tetraquark four-body potential. They also found plausible the existence of resonances in which the tetraquark component originated by a flip-flop potential is the dominant one [65].

V. SUMMARY

By using a high precision few-body calculation method, GEM, non-strange hexaquark states $q^3\bar{q}^3$ including $B_8\bar{B}_8$ and $B\bar{B}$ components are studied in flux tube models, the extended chiral quark model (Model II) and the Isgur-Karl model (Model I), with a six-body confinement potential. In the present version of flux tube models, the system will automatically choose its favorable configuration by means of the recombination of the flux tube when the quarks and antiquarks are moving. The flux tube models, which includes multibody confinement potential, generally give more attraction than the two-body confinement models with color factors that was used in the early multiquark calculations. The two types of flux tube models give similar results for non-strange hexaquark system. Our calculations suggest that some states are stable against decaying into a baryon and an anti-baryon. One gluon exchange and one boson exchange interaction also provide attractive interaction for some states, and therefore should be taken into account altogether.

The states $X(1835)$ and $X(2370)$ can be explained as $N\bar{N} + N_8\bar{N}_8$ and $\Delta\bar{\Delta} + \Delta_8\bar{\Delta}_8$ bound states in the flux tube models, the main components are compact hexaquark states $N_8\bar{N}_8$ and $\Delta_8\bar{\Delta}_8$, respectively. Such states should be color confinement resonances with three-dimensional configurations similar to a rugby ball. $X(2120)$ cannot be accommodated in this model. We admit that this analysis is based on the mass calculation only, the decay properties of these states have to be invoked to check the assignment, which is left for the future.

[1] J. Z. Bai *et al.* (BES Collaboration), Phys. Rev. Lett. **91,** 022001 (2003).

[2] M. Ablikim *et al.* (BES Collaboration), Phys. Rev. Lett. **95,** 262001 (2005).

[3] M. Ablikim *et al.* (BES Collaboration), Phys. Rev. Lett. **106,** 072002 (2011).

[4] A. Datta and P. J. O'Donnell, Phys. Lett. B **567,** 273 (2003).

[5] G. J. Ding and M. L. Yan, Phys. Rev. C **72,** 015208 (2005).

[6] C. S. Gao and S. L. Gao, Commun. Theor. Phys. **42,** 844 (2004).

[7] N. Kochelev and D. P. Min, Phys. Lett. B **633,** 283 (2006).

[8] X. G. He, X. Q. Li, X. Liu, and J. P. Ma, Eur. Phys. J. C **49,** 731 (2007).

[9] B. A. Li, Phys. Rev. D **74,** 034019 (2006).

[10] G. J. Ding and M. L. Yan, Eur. Phys. J. A **28,** 351 (2006).

[11] C. Liu, Eur. Phys. J. C **53**, 413 (2008).

[12] T. Huang and S. L. Zhu, Phys. Rev. D **73**, 014023 (2006).

[13] D. R. Entem and F. Fernández, Phys. Rev. C **73**, 045214 (2006).

[14] J. S. Yu, Z. F Sun, X. Liu, and Q. Zhao, Phys. Rev. D **83**, 114007 (2011).

[15] P. Maris and C. R. Roberts, Int. J. Mod. Phys. E **12**, 297 (2003).

[16] N. Ishii, S. Aoki, and T. Hatsuda, Phys. Rev. Lett. **99**, 022001 (2007).

[17] T. T. Takahashi and Y. Kanada-En'yo, Phys. Rev. D **82**, 094506 (2010).

[18] T. Inoue, N. Ishii, S. Aoki *et al.* (HAL QCD Collaboration), Phys. Rev. Lett. **106**, 162002 (2011).

[19] N. Ishii, AIP Conf. Proc. **1355**, 206 (2011).

[20] S. Godfrey and J. Napolitano, Rev. Mod. Phys. **71**, 1411 (1999).

[21] J. Weinstein and N. Isgur, Phys. Rev. D **41**, 2236 (1990).

[22] G. Feinberg and J. Sucher, Phys. Rev. D **20**, 1717 (1979).

[23] O. W. Greenberg and H. J. Lipkin, Nucl. Phys. **A370**, 349 (1981).

[24] J. Weinstein and N. Isgur, Phys. Rev. Lett. **48**, 659 (1982).

[25] M. Oka, Phys. Rev. D **31**, 2274 (1985).

[26] M. Oka and C. J. Horowitz, Phys. Rev. D **31**, 2773 (1985).

[27] H. J. Lipkin, Phys. Lett. B **113**, 490 (1982).

[28] O. W. Greenberg and J. Hietarinta, Phys. Lett. B **86**, 309 (1979).

[29] O. W. Greenberg and J. Hietarinta, Phys. Rev. D **22**, 993 (1980).

[30] D. Robson, Phys. Rev. D **35**, 1018 (1987).

[31] N. Isgur and J. Paton, Phys. Rev. D **31**, 2910 (1985).

[32] J. L. Ping, C. R. Deng, F. Wang, and T. Goldman, Phys. Lett. B **659**, 607 (2008).

[33] C. R. Deng, J. L. Ping, F. Wang, and T. Goldman, Phys. Rev. D **82**, 074001 (2010).

[34] F. Wang and C. W. Wong, Nuovo Cimento A **86**, 283 (1985).

[35] V. Dmitrasinovic, Phys. Rev. D **67**, 114007 (2003).

[36] C. Alexandrou, P. De Forcrand, and A. Tsapalis, Phys. Rev. D **65**, 054503 (2002).

[37] T. T. Takahashi, H. Suganuma, Y. Nemoto, and H. Matsufuru, Phys. Rev. D **65**, 114509 (2002).

[38] F. Okiharu, H. Suganuma, and T. T. Takahashi, Phys. Rev. D **72**, 014505 (2005).

[39] F. Okiharu, H. Suganuma, and T. T. Takahashi, Phys. Rev. Lett. **94**, 192001 (2005).

[40] J. L. Ping, F. Wang, and T. Goldman, Nucl. Phys. **A657**, 95 (1999).

[41] A. Valcarce, H. Garcilazo, F. Fernández, and P. González, Rep. Prog. Phys. **68**, 965 (2005).

[42] T. Goldman and S. Yankielowicz, Phys. Rev. D **12**, 2910 (1975).

[43] C. R. Deng, J. L. Ping, and F. Wang, arXiv:1202.4169.

[44] E. Hiyama, Y. Kino, and M. Kamimura, Prog. Part. Nucl. Phys. **51**, 223 (2003).

[45] N. Isgur and G. Karl, Phys. Rev. D **18**, 4187 (1978).

[46] N. Isgur and G. Karl, Phys. Rev. D **19**, 2653 (1979).

[47] N. Isgur and G. Karl, Phys. Rev. D **20**, 1191 (1979).

[48] N. Isgur and G. Karl, Phys. Rev. Lett. **48**, 659 (1982).

[49] J. Vijande, F. Fernandez, and A. Valcarce, J. Phys. G **31**, 481 (2005).

[50] J. Weistein and N. Isgur, Phys. Rev. D **27**, 588 (1983).

[51] I. T. Obukhovsky and A. M. Kusainov, Phys. Lett. B **238**, 142 (1990).

[52] F. Fernández, A. Valcarce, U. Straub, and A. Faessler, J. Phys. G **19**, 2013 (1993).

[53] A. Valcarce, P. González, F. Fernández, and V. Vento, Phys. Lett. B **367**, 35 (1996).

[54] L. Y. Glozman and D. O. Riska, Phys. Rep. **268**, 263 (1996).

[55] Y. Fujiwara, C. Nakamoto, and Y. Suzuki, Phys. Rev. C **54**, 2180 (1996).

[56] Y. Fujiwara, M. Khono, C. Nakamoto, and Y. Suzuki, Phys. Rev. C **64**, 054001 (2001).

[57] Y. Fujiwara, K. Miyagawa, M. Khono, Y. Suzuki, and C. Nakamoto, Nucl. Phys. **A737**, 243 (2004).

[58] M. D. Scadron, Phys. Rev. D **26**, 239 (1982).

[59] F. Bissey, F. G. Cao, A. R. Kitson, and A. I. Signal *et al.*, Phys. Rev. D **76**, 114512 (2007).

[60] H. X. Huang, H. R. Pang, and J. L. Ping, Mod. Phys. Lett. A **26**, 1231 (2011).

[61] J. Vijande, A. Valcarce, and J. M. Richard, Phys. Rev. D **85**, 014019 (2012).

[62] G. S. Bali, Phys. Rev. D **62**, 114503 (2000).

[63] Fan Wang, J. L. Ping, H. R. Pang, and L. Z. Chen, Nucl. Phys. **A790**, 493c (2007).

[64] S. Weinberg, *The Quantum Theory of Fields* (Cambridge University Press, Cambridge, 1995), Vol. I, p 159.

[65] P. Bicudo and M. Cardoso, Phys. Rev. D **83**, 094010 (2011).